



COULOMB FRICTION OSCILLATOR: MODELLING AND RESPONSES TO HARMONIC LOADS AND BASE EXCITATIONS

H.-K. HONG AND C.-S. LIU

Department of Civil Engineering, Taiwan University, Taipei, Taiwan

(Received 1 June 1999, and in final form 6 August 1999)

In this paper we revisit a mass–spring–friction oscillator, where the friction refers to Coulomb’s perfect dry contact friction. We refine the model formulation of the friction force and find that the equation of motion of the oscillator is a two-phase linear system with a slide–stick switch, rather than the usual three-phases equations. Also we obtain a simple slide–slide condition. Then the exact solution of the response to simple harmonic loading is obtained. With the aid of the long-term behavior of the exact solution, the steady motions of the oscillator with 0, 1, 2, 4, 6, 8, 10, 12, 14 stops per cycle are categorized in the parametric space of the ratios of forces and frequencies. Stops of zero duration are further classified into two types: normal stops and abnormal stops, the criteria of which are also given.

© 2000 Academic Press

1. INTRODUCTION

The study of non-linear, hysteretic behavior of mechanical systems has been of great interest to engineers and researchers in a variety of engineering fields, since many engineering systems exhibit hysteretic behavior under cyclic loading. A survey of various non-linear oscillators was given in, for example, Nayfeh and Mook [1]. In this paper, we study a single-degree-of-freedom oscillator with the parallel presence of a linear spring and a Coulomb friction device, which is subjected to external loading or base excitation. A schematic drawing is given in Figure 1 displaying a mass–spring system with the mass possibly sliding against a dry surface when subjected to an external load $p(t)$.

The equation of motion of the oscillator is

$$m\ddot{x}(t) + k[x(t) - x_{eq}] + r_a(t) = p(t), \quad (1)$$

where a superposed dot represents time differentiation: x , \dot{x} , \ddot{x} and m are the position co-ordinate, velocity, acceleration and mass, respectively, of the body of the oscillator; k is the stiffness of the spring; x_{eq} is the (static equilibrium) position of the body of the oscillator at which the spring is not stretched so that the spring force is zero; r_a is the friction force acting in a direction opposite to the direction of the

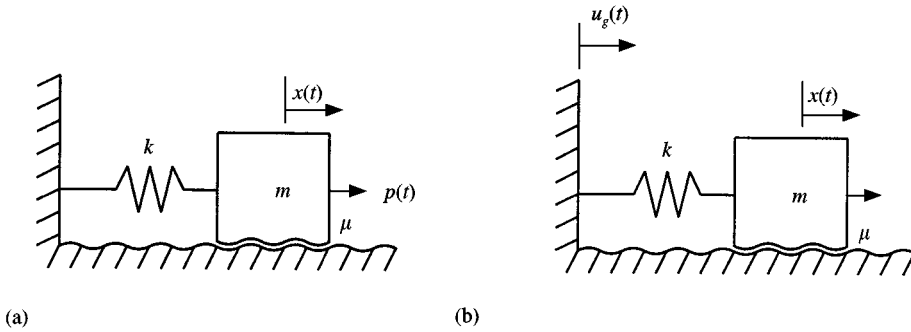


Figure 1. The mass–spring–friction oscillator, where the friction refers to Coulomb’s perfect dry friction between the mass and the ground surface: (a) mass excitation, (b) base excitation.

motion;[†] and $p(t)$ denotes external loading. If the mass is subjected to a base translation $u_g(t)$, as shown in Figure 1(b), the equation of motion may be recast to the same equation (1) by letting $p(t) = ku_g(t)$ and re-designating x , \dot{x} , \ddot{x} , to be relative to the base. Thus, the slight difference between the mass excitation as in Figure 1(a) and the base excitation as in Figure 1(b) will henceforth in this paper be seldom mentioned again.

As early as in 1931, Den Hartog [2] presented a closed-form solution for the steady state zero-stop response of a harmonically excited oscillator with Coulomb’s friction. Since then more contributions to this vibration issue have been made [3–12]. Nevertheless, if attention is focused on the friction force itself instead of the whole equation of motion, it is found that even the simplest case, the Coulomb perfect dry contact friction, still lacks an accurate and complete mathematical expression. To precisely formulate the constitutive law for the friction force r_a , the old issue of the modelling of Coulomb’s perfect dry contact friction is reconsidered in Section 2. The conditions for sliding and sticking and their respective governing equations of motion are formulated in Section 3, and then the exact solutions of the responses to simple harmonic loading are obtained in Section 4. Also in Section 4, the responses are classified according to the number of stops per cycle of the steady state response.

2. MODELLING FRICTION

The following expression

$$r_a = \begin{cases} r_y & \text{if } \dot{x} > 0, \\ -r_y & \text{if } \dot{x} < 0 \end{cases} \quad (2, 3)$$

is usually used to represent the two-valuedness of Coulomb’s perfect dry contact friction, as shown in Figure 2(a). It is assumed that r_y , m and k are positive constants

[†]Generally speaking, for formulating dynamic equations (Newton’s law, equation (1)) every kind of constitutive forces (e.g., the spring force, viscous force, friction force) is opposite to the direction to motion (including x , \dot{x} , \ddot{x}); however, for formulating constitutive equations (Coulomb’s law, equations (2,3) or (7–9) or (10–13)) the constitutive forces are in the same directional sense as the motion.

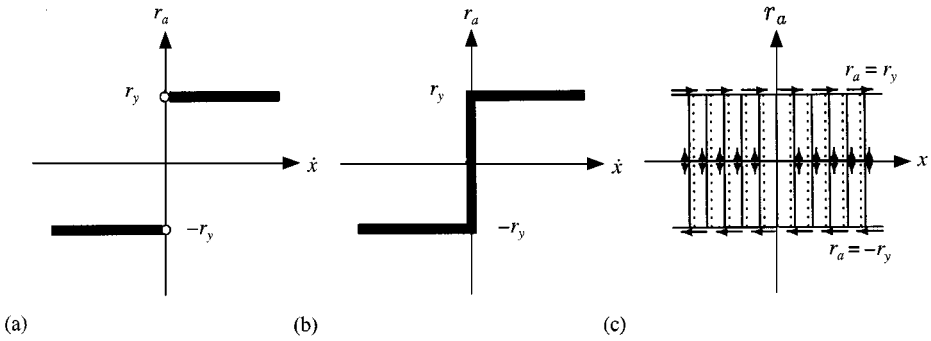


Figure 2. The relation between the friction force r_a and velocity \dot{x} : (a) two-valued representation, (b) multiple-valued representation: (c) the relation of the friction force r_a and displacement x .

to be determined experimentally,

$$m > 0, \quad k > 0, \quad r_y > 0. \tag{4-6}$$

If the contact surfaces are horizontal on the earth ground, $r_y = \mu mg$, where g is the acceleration due to gravity and μ is the coefficient of friction. This formalism is correct but incomplete; equations (2, 3) are good for the sliding motion but contain no information about sticking. In fact, the friction force r_a may take any[‡] value between $-r_y$ and r_y where $\dot{x} = 0$; therefore, the following expression provides a more precise description:

$$r_a \begin{cases} = r_y & \text{if } \dot{x} > 0 \\ \in [-r_y, r_y] & \text{if } \dot{x} = 0, \\ = -r_y & \text{if } \dot{x} < 0. \end{cases} \tag{7-9}$$

Figure 2(b) depicts its graphical representation. Notice the distinction between the two-valuedness of r_a in equations (2, 3) and Figure 2(a) and the multiple-valuedness of r_a in equations (7-9) and Figure 2(b). It can be seen that the equation of motion has *three* phases upon substituting equations (7-9) for r_a in equation (1).

Nevertheless, the formalism (7-9), although correct, is not complete yet, since it still lacks a two-way relation between \dot{x} and r_a . For completeness, we need a flow rule (10) and complementary trios (11)-(13) as follows:

$$\dot{x} = \frac{\dot{\Lambda}}{r_y^2} r_a, \quad |r_a| \leq r_y, \quad \dot{\Lambda} \geq 0, \quad |r_a| \dot{\Lambda} = r_y \dot{\Lambda}, \tag{10-13}$$

where $\dot{\Lambda}$ is the friction power, so that Λ is the dissipated energy due to friction. According to this formulation, the relation of r_a and x is schematically shown in

[‡]This is for formulating constitutive equations. For formulating dynamics equations, the friction force takes on a certain definite value that should balance the other forces within the range $[-r_y, r_y]$.

Figure 2(c),[§] which can be seen to convey more information than Figure 2(b). It is not difficult to verify that equations (10)–(13) imply equations (7–9), but conversely that equations (7–9) do not suffice to lead to equations (10)–(13).

Proof. Given equations (10)–(13), we first consider the first case of equations (7–9): the condition $\dot{x} > 0$ leads to $\dot{\Lambda}r_a > 0$ via equation (10) and (6). Then it follows from inequality (12) that $\dot{\Lambda} > 0$ and $r_a > 0$. Further by equation (13) it should be $|r_a| = r_y$ and then $r_a = r_y$. Second, let us consider the second case: the condition $\dot{x} = 0$ implies that $r_a = 0$ or $\dot{\Lambda} = 0$ in view of equations (10) and (6). Either one complies with $-r_y \leq r_a \leq r_y$ of inequality (11). Finally, consider the third case: the condition $\dot{x} < 0$ implies $\dot{\Lambda}r_a < 0$ by the same token, and then $\dot{\Lambda} > 0$ and $r_a < 0$ by inequality (12), and then $r_a = -r_y$ by equation (13). Summarizing the above three cases, we conclude that equations (10)–(13) imply equations (7–9).

Conversely, if starting from equations (7–9), one has no information about the relation among r_a , \dot{x} and $\dot{\Lambda}$. Therefore, equations (7–9) are not sufficient to derive equations (10), (12) and (13). \square

A significant merit of equations (10)–(13) is that they can be easily extended to two or more dimensions, as shown in Appendix A, so that *consistent* n -dimensional friction models with $n = 1, 2, 3, \dots$ are available.

In view of equation (1), the constitutive force[¶] $r(t)$ of the oscillator can be defined as

$$r = r_a + r_b \quad (14)$$

with r_a modelled by equations (10)–(13) and r_b by

$$r_b(t) = k[x(t) - x_{eq}],$$

or in rate form

$$\dot{r}_b = k\dot{x}. \quad (15)$$

Thus, the relation between the constitutive force function $r(t)$ and the position co-ordinate function $x(t)$ is described by equations (10)–(15), which may be schematically illustrated in Figure 3(a). Equation (10) is a flow rule, giving a two-way relation between the velocity \dot{x} and the friction force r_a via a proportional multiplier equal to the friction power $\dot{\Lambda}$ divided by the friction bound squared r_y^2 . Equation (11) specifies an admissible range of the friction force. Equation (12) forbids a negative friction power, so that the velocity is either zero or in the same directional sense as that of friction force (see footnote[†]). Equation (13) allows either $\dot{\Lambda} = 0$ (the sticking phase) or $|r_a| = r_y$ (the sliding phase). Equation (14)

[§]The explanations of the precise meanings of the solid and dotted vertical lines as in Figures 2(c), 3(a), 6(c) and 6(g) are relegated to section 3.4.

[¶]The constitutive force is a convenient term used sometimes to refer *grossly* to the spring force, viscous force, friction force, etc. It may be called the restoring force, or some other appropriate term.

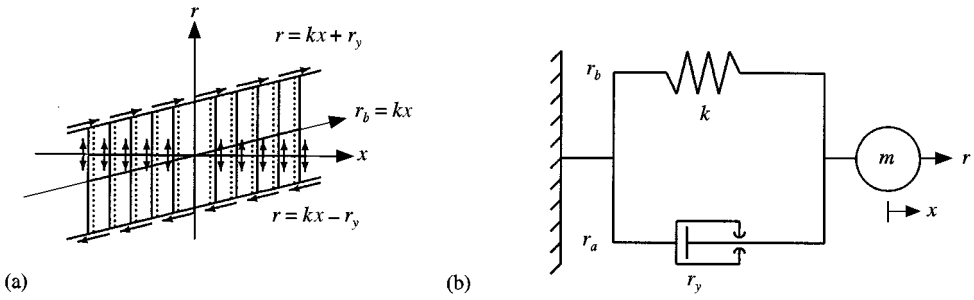


Figure 3. (a) The relation between the constitutive force r and displacement x , (b) arrangement of mechanical elements.

is the decomposition of the constitutive force. Equation (15) is a linearly (hypo)elastic law for the spring force. The mechanical-elements arrangement displayed in Figure 3(b) may help illustrate the mechanisms implied in Figure 1 and help explain the meanings of the constitutive equations (10)–(15).

Notice in passing that the model of equations (10)–(15) is a special case of the bilinear elastoplastic model discussed by Liu [13], which has been used intensively in the analyses of isolation systems of buildings and equipment in recent years. See, for example, Skinner *et al.* [14], where the bilinear model describing the relation between the constitutive force and the relative velocity of the two end-plates of a seismic isolator was combined with the equation of motion to simulate the hysteretic motion and dissipation capacity of the isolator.

3. SLIDING AND STICKING

3.1. TWO PHASES

The complementary trios (11–13) imply there are precisely *two phases*: (1) $\dot{\Lambda} > 0$ and $|r_a| = r_y$, (2) $\dot{\Lambda} = 0$ and $|r_a| \leq r_y$. The complementary trios can be interpreted as the heavy two-segment line in Figure 4(a), and in Figure 4(b) the two phases are further distinguished as the two segments of the two-segment line. It cannot be overemphasized that among equations (10–15) the key of precisely two phases is equation (13).

For phase (1), $\dot{\Lambda} > 0$ and $|r_a| = r_y$, so $\dot{\Lambda} = r_a \dot{x} > 0$ by equation (10). For phase (2), $\dot{\Lambda} = 0$ and $|r_a| \leq r_y$, so $\dot{x} = 0$ by equation (10) and then $\dot{\Lambda} = r_a \dot{x} = 0$. Therefore, the friction power formula

$$\dot{\Lambda} = r_a \dot{x}$$

holds for the two phases.

Phase (1) is nothing but the *sliding phase*, since $\dot{\Lambda} = r_a \dot{x} > 0$ means $\dot{x} \neq 0$ so that the contact surfaces slide relative to each other and dissipation occurs due to friction between the sliding surfaces. Phase (2) is obviously the *sticking phase*, since $\dot{\Lambda} = 0$ drastically reduces equation (10) to $\dot{x} = 0$, which indicates that the contact surfaces are sticking. In the sliding phase, the sliding friction causes positive dissipation and the oscillator exhibits hysteretic behavior, while in the sticking

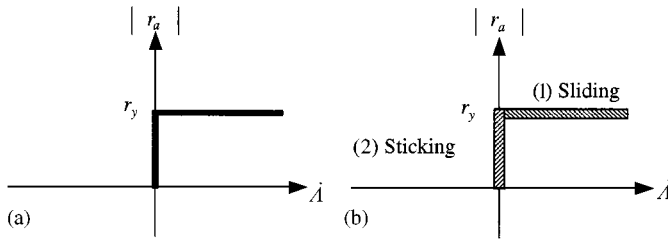


Figure 4. The complementary trios (11–13) appear as (a) a two-segment line composed of (b) two segments: (1) the sliding phase $\{\dot{A} > 0 \text{ and } |r_a| = r_y\}$ and (2) the sticking phase $\{\dot{A} = 0 \text{ and } |r_a| \leq r_y\}$.

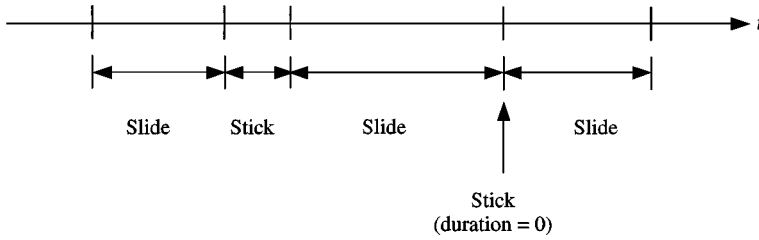


Figure 5. A typical motion with the time intervals of slide–stick–slide and slide–slide with a zero-duration stop.

phase the oscillator is at rest and no dissipation occurs. Thus, the history of the motion of the friction oscillator may be composed of a succession of contiguous time intervals (see Figure 5), sliding-phase intervals being interlaced with sticking-phase intervals, but the time duration of a sticking-phase interval can be finite, infinite (permanent sticking, shakedown), or zero (see section 3.4).

3.2. THE SLIDING PHASE

In this section and the following, we derive the governing equations for the two phases, which will soon be seen to be expressed in terms of not only the displacement function $x(t)$ but also the restoring force function $r(t)$. In terms of $r(t)$, equation (1) changes to

$$m\ddot{x}(t) + r(t) = p(t). \tag{16}$$

It follows from equations (14) and (15) that

$$r(t) = r(t_i) + r_a(t) - r_a(t_i) + k[x(t) - x(t_i)] \tag{17}$$

for the two time instants t and t_i . Substituting equation (17) for r into equation (16), we have

$$m\ddot{x}(t) + kx(t) + r_a(t) = p(t) - r(t_i) + r_a(t_i) + kx(t_i). \tag{18}$$

In the sliding phase, $|r_a| = r_y$, and so in a sliding-phase interval $\dot{r}_a = 0$, that is,

$$r_a(t) = r_a(t_i), \quad (19)$$

where the initial time t_i is chosen to be the start-to-slide time t_{slide} of the sliding-phase interval under consideration. Hence, equation (18) can be simplified to

$$m\ddot{x}(t) + kx(t) = p(t) - r(t_i) + kx(t_i). \quad (20)$$

With the constitutive force on the right-hand side, this equation should be supplemented by

$$r(t) = r(t_i) + k[x(t) - x(t_i)] \quad (21)$$

which is equation (17) but with equation (19) taken into account. Equations (20) and (21) together are the sliding-phase governing equations for $x(t)$ and $r(t)$. They are coupled.

3.3. THE STICKING PHASE

In a sticking-phase interval, $\dot{A} = 0$, and so by equations (6), (10) and (15) we have

$$r_b(t) = r_b(t_i), \quad (22)$$

$$x(t) = x(t_i), \quad (23)$$

where the initial time t_i is now chosen as the start-to-stick time t_{stick} of the sticking-phase interval. In view of equations (16) and (23), the constitutive force is given by

$$r(t) = p(t). \quad (24)$$

Equations (23) and (24) together are the sticking-phase governing equations for $x(t)$ and $r(t)$. They are uncoupled.

The above analysis shows that the oscillator is described by the linear equations (23) and (24) during the sticking phase, but governed by the linear differential equations (20) and (21) in the sliding phase. Hence, it is a two-phase linear system with a slide-stick switch.

3.4. THE SLIDE-SLIDE CONDITION

It is interesting to find the condition under which the time duration of a sticking-phase interval to be zero. The transition (say at time t) from a sliding-phase interval to a sticking-phase interval of non-zero time duration (a solid vertical line in Figures 2(c), 3(a), 6(c) and 6(g)) is possible only if $|p(t) - kx(t)| < r_y$. Otherwise, a sliding-phase interval will jump to another

sliding-phase interval with a sticking phase of zero time duration (a dotted vertical line in Figures 2(c), 3(a), 6(c) and 6(g)) present in between the two sliding-phase intervals, but both the sliding-phase intervals are modelled by the same governing equations.

If at the time instant t

$$|p(t) - kx(t)| \geq r_y, \quad (25)$$

the duration of the sticking-phase interval is zero (such an interval is referred to later on as a zero-duration stop), resulting in the oscillator jumping from a sliding-phase interval to another sliding-phase interval. Therefore, equation (25) may be called the slide-slide condition. Note that condition (25) is much simpler than that proposed by Makris and Constantinou [11].

4. RESPONSE TO HARMONIC LOADING

In what follows, the driving force is taken to be simple harmonic with a single driving (angular) frequency ω_d ,

$$p(t) = p_0 \sin \omega_d t = k u_{g0} \sin \omega_d t, \quad (26)$$

where p_0 is the amplitude of the periodic force acting on the mass, and u_{g0} is the amplitude of the periodic base excitation.

4.1. EXACT SOLUTION

To input (26) the response in the sliding phase can be obtained by solving equations (20), (21) and (26) as follows:

$$\begin{aligned} x(t) = & x(t_i) + \frac{\dot{x}(t_i)}{\omega_n} \sin \omega_n(t - t_i) - \frac{r(t_i)}{k} [1 - \cos \omega_n(t - t_i)] \\ & + A [\sin \omega_d t - \cos \omega_n(t - t_i) \sin \omega_d t_i - \Omega \sin \omega_n(t - t_i) \cos \omega_d t_i], \quad (27) \end{aligned}$$

where $\omega_n := \sqrt{k/m}$ is the natural frequency, and

$$A := \frac{p_0}{k(1 - \Omega^2)}, \quad \Omega := \frac{\omega_d}{\omega_n}. \quad (28, 29)$$

Instead of the usual two formulas (one for $\dot{x} > 0$ and the other for $\dot{x} < 0$; see, for example, equations (4) and (5) in reference [11]), the exact solution (27) consists of only one formula. Containing the constitutive force on the right-hand side, equation (27) should be supplemented by equation (21). In the sticking phase the response is simply given by equations (23) and (24).

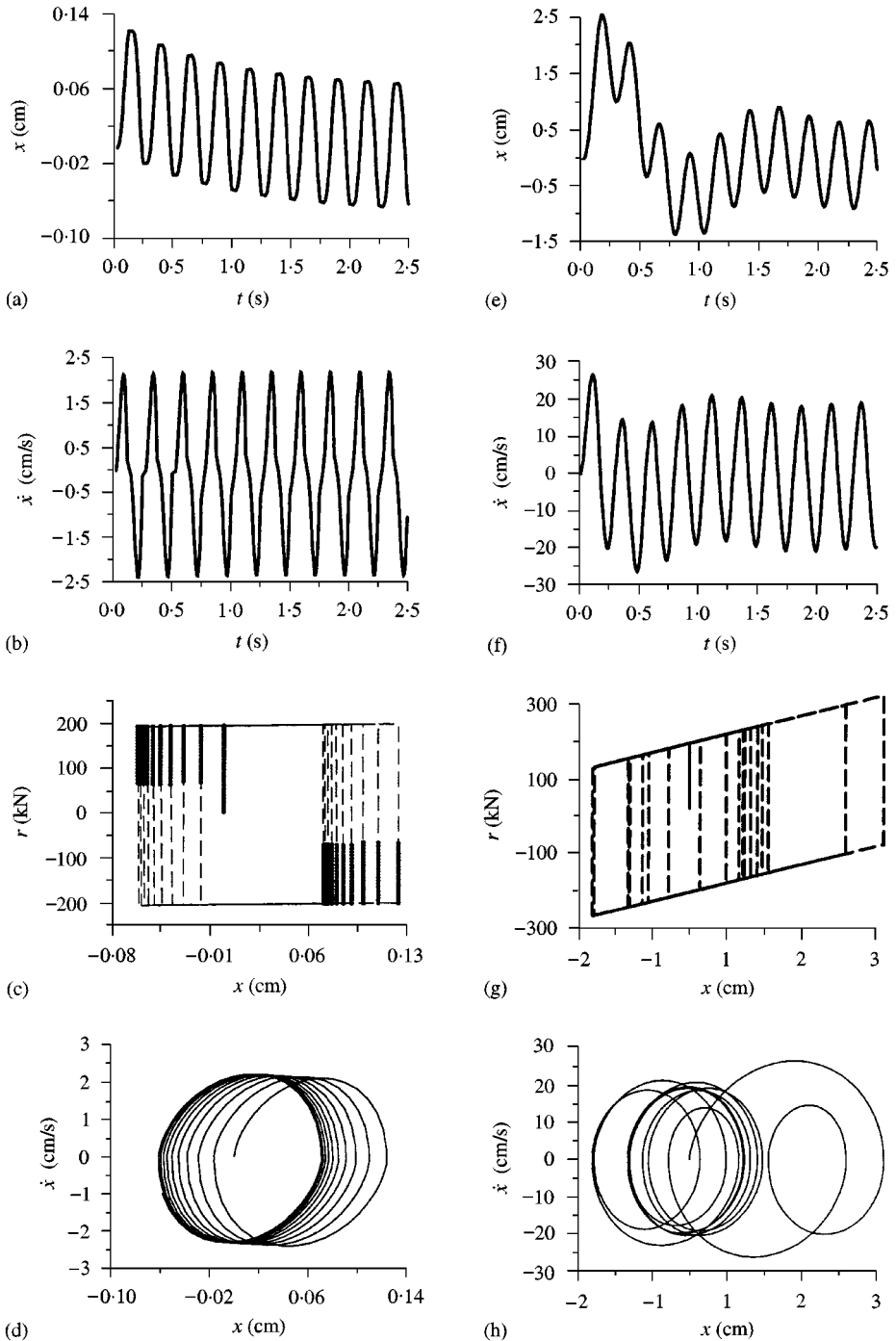


Figure 6. Two typical responses of the mass–spring–friction oscillator with sticking of (a)–(d) under smaller driving force and sliding of (e)–(h) under larger driving force.

Some results about the responses are shown in Figure 6, in which the parameters used were $m = 200 \text{ kN s}^2/\text{m}$, $k = 5000 \text{ kN/m}$, $r_y = 200 \text{ kN}$, $\omega_d = 8\pi \text{ rad/s}$ and $p_0 = ku_{g0} = 300 \text{ kN}$ for (a)–(d) and $p_0 = ku_{g0} = 1000 \text{ kN}$ for (e)–(h).

4.2. THE START-TO-STICK TIME

Since a sliding-phase interval is switched off at the same instant when a sticking-phase interval is switched on, the start-to-stick time t_{stick} of the sticking-phase interval is the end time of the sliding phase, which is determined by solving $\dot{x}(t) = 0$ for $t = t_{stick}$ with the $x(t)$ given by equation (27). The resulting is a transcendental equation, and so a numerical method may be invoked to calculate the start-to-stick time.

4.3. THE START-TO-SLIDE TIME

Owing to simplicity in the sticking-phase equations, the start-to-slide time $t = t_{slide}$, which is the end time of the preceding sticking-phase interval, can be determined exactly by solving

$$|p_0 \sin \omega_d t_{slide} - kx(t_i)| = r_y.$$

For this purpose, let us define two bounds of the ratio $r(t_i)/p_0$:

$$b_1 := \frac{kx(t_i) + r_y}{p_0}, \quad b_2 := \frac{kx(t_i) - r_y}{p_0}, \quad b_1 > b_2,$$

where t_i is the initial time of the sticking-phase interval under investigation. Dividing the values of b_1, b_2 into seven cases (see (a)–(g) in Figure 7), we have the start-to-slide time formulae:

$$t_{slide} = \begin{cases} t_i & \text{if } b_1 > 1 \text{ and } b_2 < -1 & \text{(a),} \\ \infty & \text{if } b_1 < -1 \text{ or } b_2 > 1 & \text{(b),} \\ \frac{\arcsin b_1}{\omega_d} & \text{if } 0 < b_1 \leq 1 \text{ and } b_2 < -1 & \text{(c),} \\ \frac{\arccos b_1}{\omega_d} & \text{if } b_2 < -1 \leq b_1 \leq 0 & \text{(d),} \\ \frac{\arcsin b_2}{\omega_d} & \text{if } 0 < b_2 \leq 1 < b_1 & \text{(e),} \\ \frac{\arccos b_2}{\omega_d} & \text{if } b_1 > 1 \text{ and } -1 \leq b_2 \leq 0 & \text{(f),} \\ \min(t_1, t_2) & \text{if } -1 \leq b_2 < b_1 \leq 1 & \text{(g),} \end{cases} \quad (30-36)$$

where

$$t_j = \begin{cases} \frac{\arcsin b_j}{\omega_d} & \text{if } b_j > 0, \\ \frac{\arccos b_j}{\omega_d} & \text{if } b_j < 0 \end{cases}$$

for $j = 1, 2$. In the above formulae, the values of arcsin and arccos should be taken such that $t_i \leq t_{slide} < t_i + 2\pi/\omega_d$. Case (a) is nothing but the case of zero-duration stop (see Figure 5), that is, the case satisfying the slide–slide condition (25), while case (b) is the case of permanent sticking.

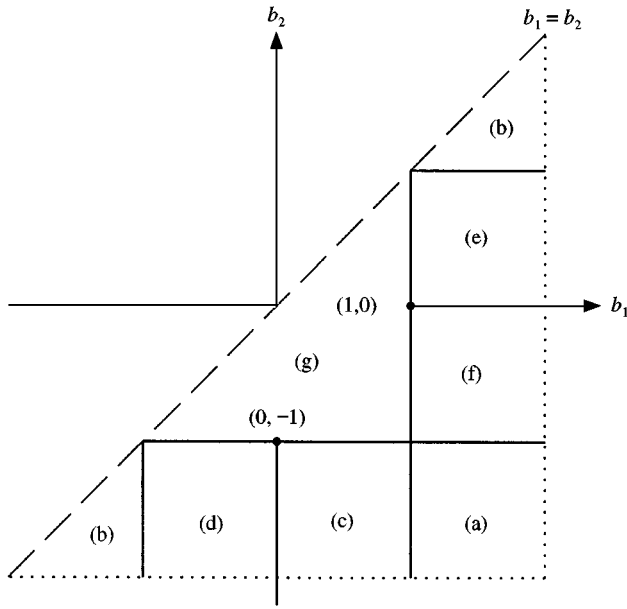


Figure 7. The determination of the start-to-slide time should consider seven cases.

4.4. CLASSIFICATION OF THE STEADY-STATE BEHAVIOR

It is known from the exact solution obtained above and evidenced in, for example, Figures 6(d) and 6(h) that the response of the harmonically excited oscillator even with the presence of friction tends to steady periodic motion in the long run. The motion is said to be in steady state. In fact, in many occasions especially for engineering design purposes, we are often more concerned with the steady-state response rather than the transient response. Since one of the most notable features of the friction oscillators is sticking, we may classify in a space of parameters the long-term steady state behavior by the number of stops per cycle of the simple harmonic driving force. In view of the five constants m, k, r_y, p_0, ω_d that we have, let us define the force ratio

$$\alpha := \frac{p_0}{r_y}$$

and the frequency ratio

$$\Omega := \omega_d / \omega_n = \omega_d / \sqrt{k/m}.$$

Thus, it is clear that the two dimensionless parameters $(1/\alpha, \Omega)$ play the role of classifying the steady state behavior.

Based on a study of 2500 ($= 50 \times 50$) cases, we found that there were many types of steady-state behavior: permanent sticking, zero stop per cycle (i.e., non-sticking oscillation), one stop per cycle, two stops per cycle, four stops per cycle, six stops per cycle, and so on. In Figure 8, the distribution of these types of behavior is

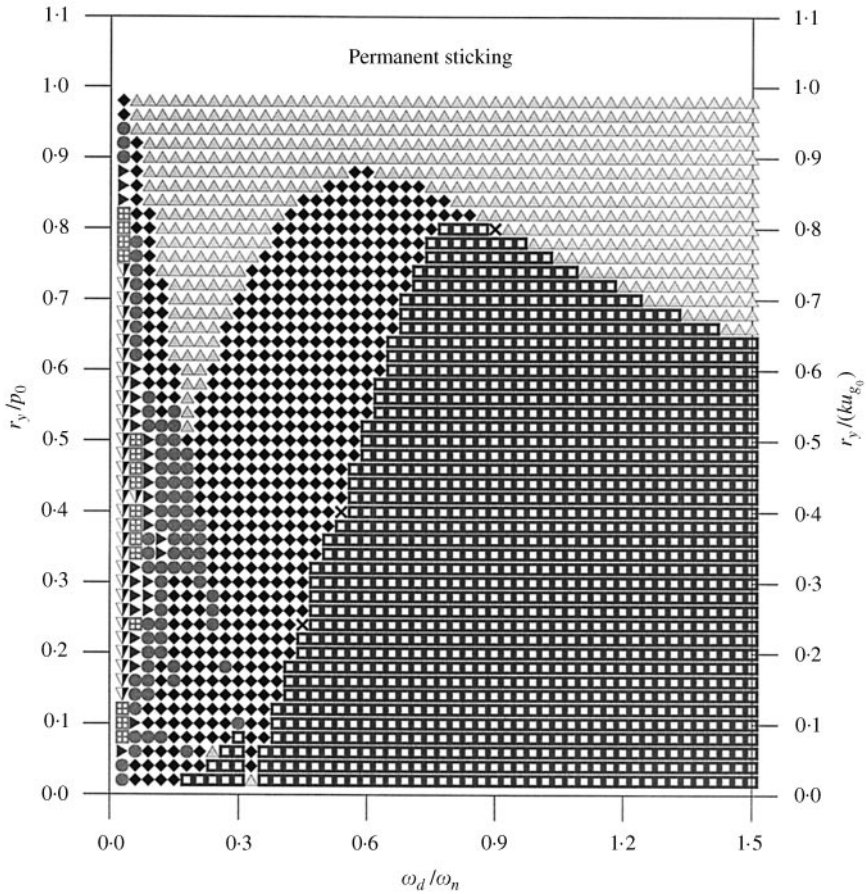


Figure 8. The distribution of the nine types of motions: permanent sticking, zero stop per cycle (i.e., non-sticking oscillation) one stop per cycle and 2, 4, 6, 8, 10 and more stops per cycle in the parametric plane $(1/\alpha, \Omega)$. $1/\alpha = r_y/p_0$, $\Omega = \omega_d/\omega_n$: \square , zero stop; \times , one stop; \triangle , two stops; \blacklozenge , four stops; \bullet , six stops; \blacktriangleright , eight stops; \blacksquare , ten stops; \blacktriangledown , more stops.

plotted in the plane $(1/\alpha, \Omega)$ in the ranges of $0 < 1/\alpha < 1.1$ and $0 < \Omega < 1.5$. The blank part of this plot represents the permanent sticking type. It is seen that most of the motions had zero or a small even number of stops per cycle, and only a small number of motions had higher even numbers of stops per cycle, the pattern of the distribution being rather complicated. Notice that there were three cases among the 2500 cases which had one stop per cycle. Figure 9 provides a finer view in the range of $0.4 < 1/\alpha < 1.0$ and $0 < \Omega < 0.1$, in which most cases had more than 10 stops per cycle for $\Omega < 0.04$ (i.e., when the driving frequency is rather small if compared with the natural frequency).

The responses are demonstrated in Figures 10 and 11, with the parameters $1/\alpha = 0.7$ and $\Omega = 1.2$ for Figure 10 and $1/\alpha = 0.7$ and $\Omega = 0.03$ for Figure 11. The period $2\pi/\omega_d$ of the simple harmonic input was taken to be 1 s for the calculations. In the plots the sliding motion is represented by the thin line while the sticking one is marked by the black heavy line. As shown in Figure 10, each of the first three

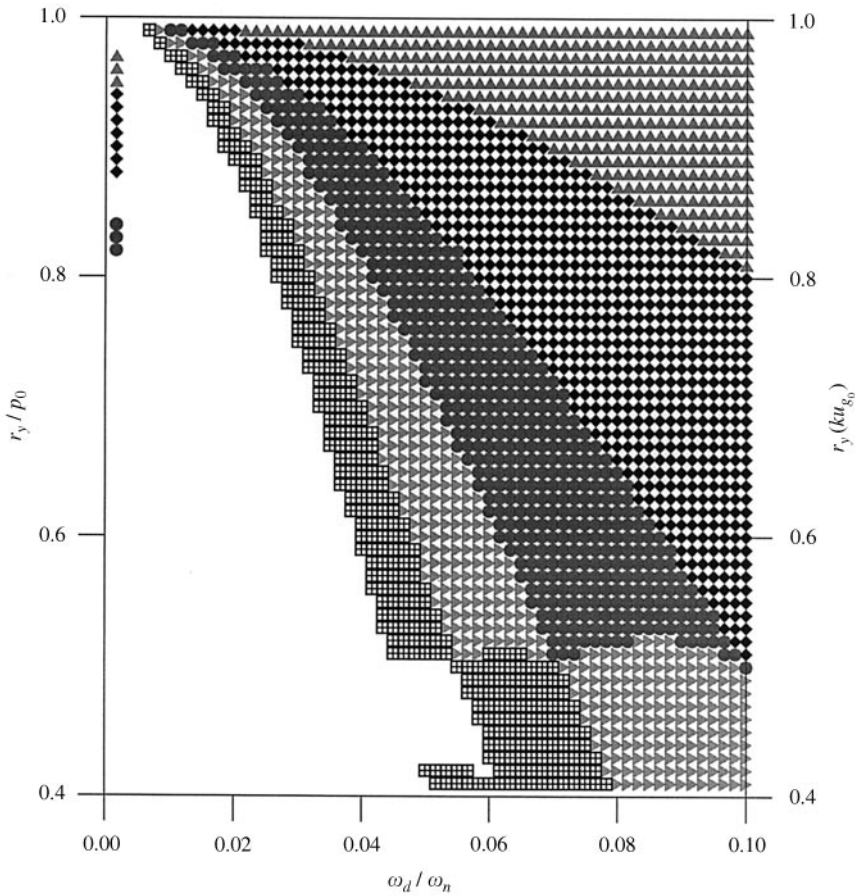


Figure 9. A more refined version of the distribution of the types of motions. $1/\alpha = r_y/p_0$, $\Omega = \omega_d/\omega_n$: \blacktriangle , two stops, \blacklozenge , four stops; \bullet , six stops; \blacktriangleright , eight stops; \blacksquare , ten stops; \blacktriangledown , more stops.

cycles had two stops, but the time durations of the stops tended to diminish. After those the fourth cycle had one stop and all the following cycles had zero stop. It was as late as about the 10th cycle a stabilized loop in the phase plane (x, \dot{x}) was obtained (see Figure 10). Therefore, the steady state response for $(1/\alpha, \Omega) = (0.7, 1.2)$ must be classified as zero stop per cycle (see Figure 8), not as two stops or one stop per cycle. Similarly, for the case of Figure 11 there were 10 stops in the first cycle but 12 stops in each of the following cycles,^{||} and so steady state behavior of $(1/\alpha, \Omega) = (0.7, 0.03)$ must be classified as 12 stops per cycles. The loop of the steady state in the phase plane was still simple and closed (see Figure 11), but it was much more complicated than that of Figure 10. For illustration we select and display in Figure 12 eight typical types of steady-state behavior: zero stop per cycle with parameters $(1/\alpha, \Omega) = (0.6, 1.8)$, two stops per cycle with $(0.9, 1.5)$, four stops per cycle with $(0.6, 0.105)$, six stops per cycle with $(0.75, 0.06)$, eight stops per cycle with $(0.85, 0.03)$, 10

^{||} For clarity and space saving only the first, fourth, 10th and 15th cycles are shown.

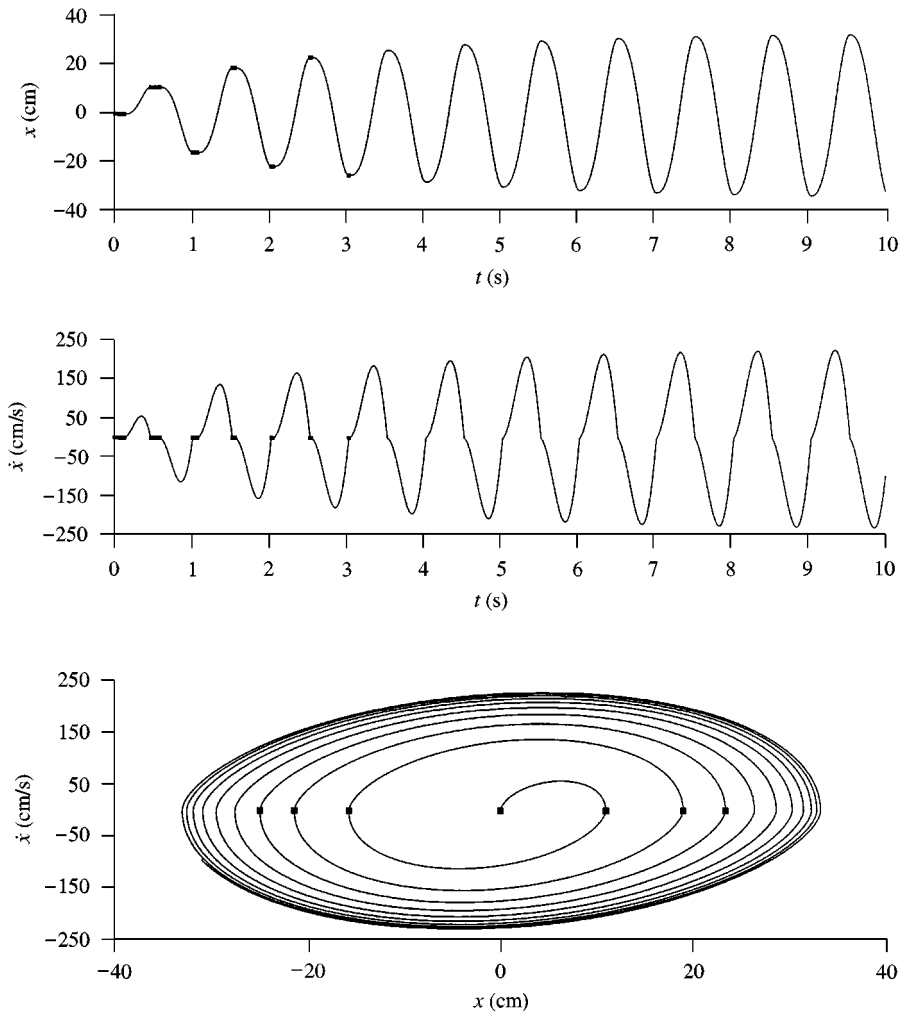


Figure 10. An example with $1/\alpha = 0.7$ and $\Omega = 1.2$ to demonstrate the steady motion, where the time duration of the stops are gradually diminished to zero after the fifth cycle, so in its steady state the motion is zero stop per cycle.

stops per cycle with $(0.8, 0.03)$, 12 stops per cycle with $(0.7, 0.03)$, and 14 stops per cycle with $(0.576, 0.03)$. It can be seen that the number of stops per cycle is equal to the number of humps in the phase plane (x, \dot{x}) and to the number of humps in the velocity history (t, \dot{x}) .

4.5. MAGNIFICATION FACTORS

In a steady-state response analysis, we merely want to know the maximum values and the phase lags of the steady state responses, for those values convey crucial information about the oscillator and help us understand its main behavior. For these let us define the magnification factor of displacement and the magnification

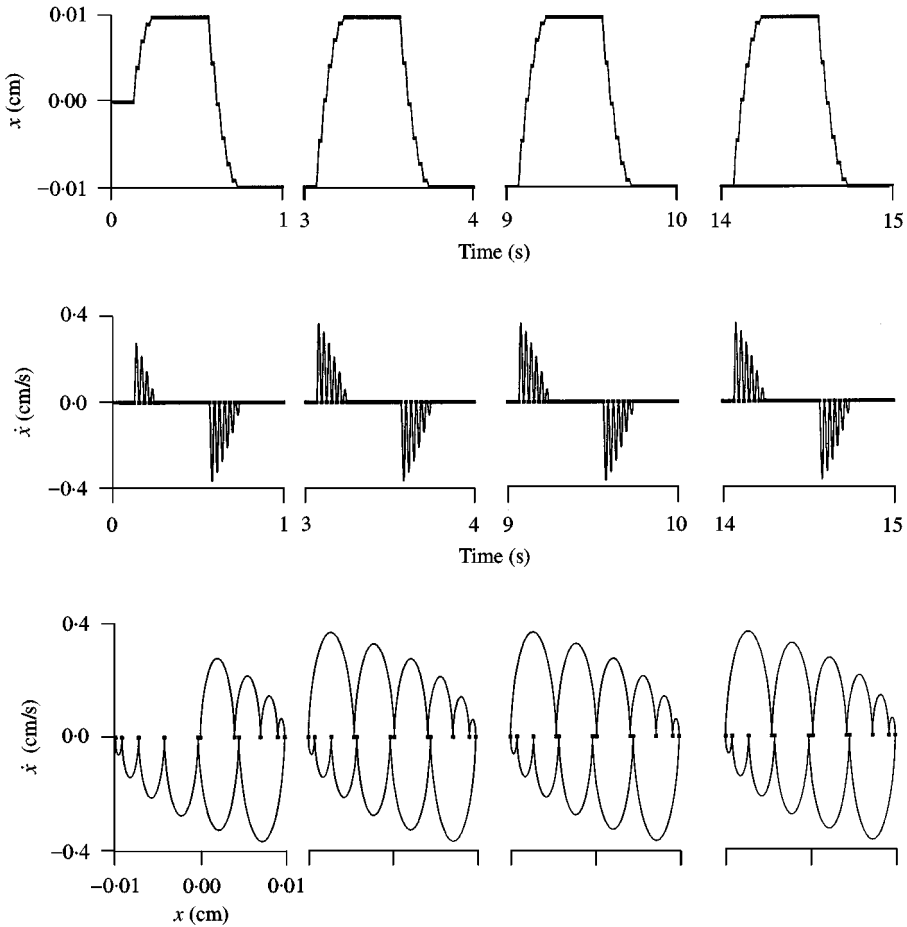


Figure 11. An example with $1/\alpha = 0.7$ and $\Omega = 0.03$ to demonstrate the steady motion, where initially it is 10 stops per cycle, but in its steady state the motion is 12 stops per cycle.

factor of velocity, respectively, as follows:

$$\Delta_{mf} := \frac{k\Delta_0}{p_0}, \quad V_{mf} := \frac{kV_0}{\omega_d p_0}, \quad (37, 38)$$

where Δ_0 and V_0 denote the maximum displacement and the maximum velocity, respectively, in the steady state. In Figure 13 the variations of these two factors with respect to the frequency ratio Ω are shown for $1/\alpha = 0.1, 0.2, 0.3, 0.4, 0.5$ and 0.6 . For $\Omega = 1$ resonance occurs for all α , and both Δ_{mf} and V_{mf} tend to infinity.

4.6. NORMAL STOPS VERSUS ABNORMAL STOPS

Stops with zero duration may be further classified into two types [11]: normal stop and abnormal stop. The former occurs when the displacement reaches a local

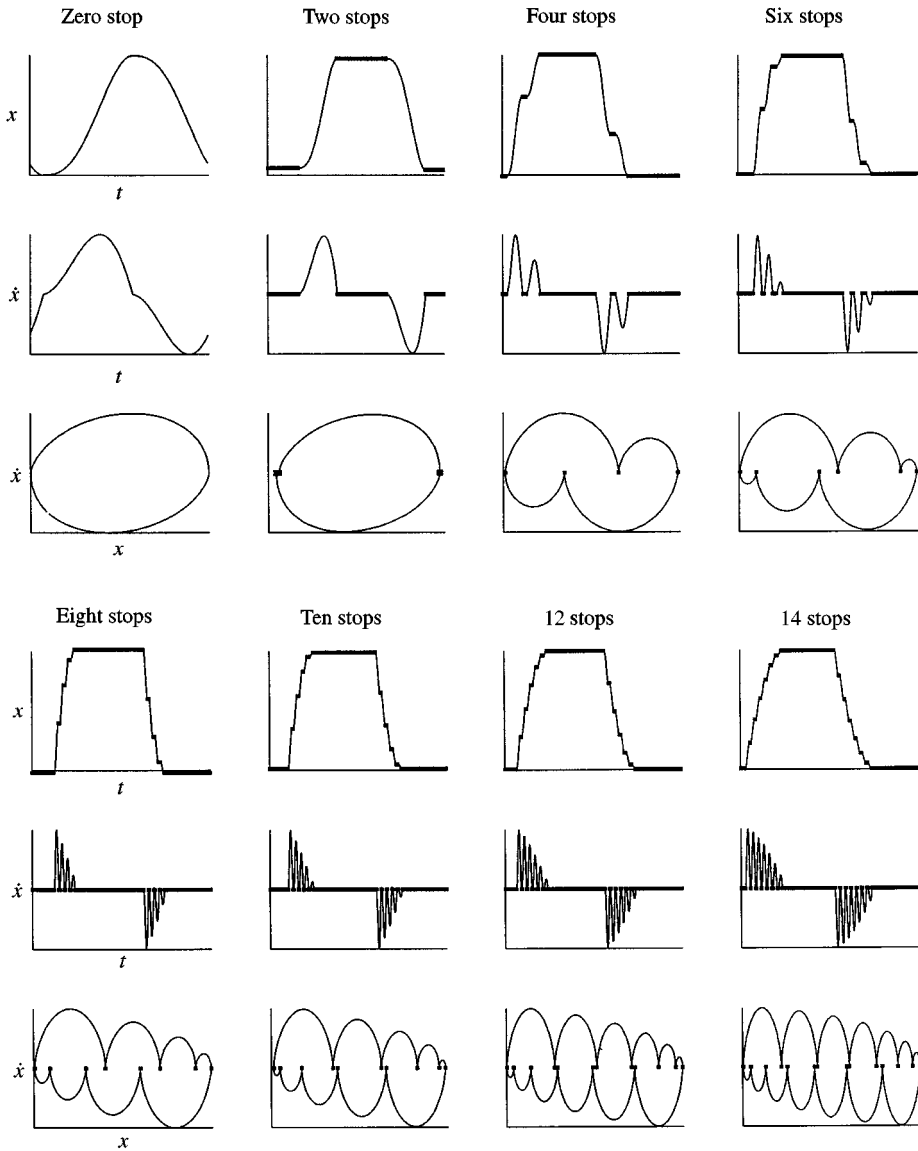


Figure 12. Illustration of the typical behavior of various numbers of stops per cycle in the steady state.

extremum and the mass reverses its direction of motion at a turning point. The criteria for the normal stop are

$$|p(t) - kx(t)| \geq r_y \quad \text{and} \quad r_a(t)\ddot{x}(t) < 0 \tag{39}$$

at the time moment t with $\dot{x}(t) = 0$. The abnormal stop occurs when the displacement is less than its local extremum and, upon separation, the mass moves in the same direction as its motion prior to the stop. The criteria for the abnormal

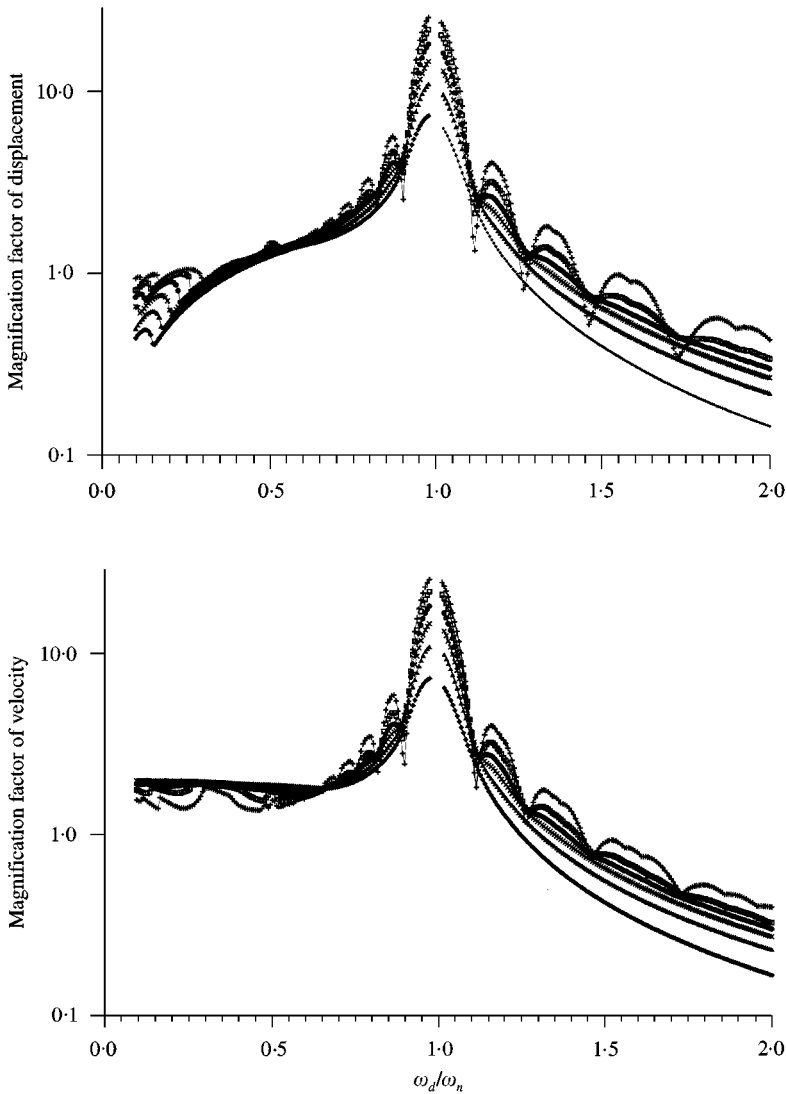


Figure 13. The variations of the magnification factors with respect to the frequency ratio for several values of the force amplitude ratio α . $1/\alpha = r_y/p_0$, $\Omega = \omega_d/\omega_n$: $-+-$, $r_y/p_0 = 0.1$; \square , 0.2 ; $--\bullet-$, 0.3 ; \times , 0.4 ; \blacktriangle , 0.5 ; $-\blacklozenge-$, 0.6 .

stop are

$$|p(t) - kx(t)| \geq r_y \quad \text{and} \quad r_a(t)\ddot{x}(t) > 0. \tag{40}$$

In Figure 14 the two types of motions are demonstrated with the help of their local time histories of displacement and velocity and the curves in the phase plane (x, \dot{x}) . The control parameters which allow the occurrence of zero-duration stops with normal or abnormal types are displayed in Figure 15. The number of abnormal stops is counted within one cycle of the periodic steady state. For each Ω fixed, the

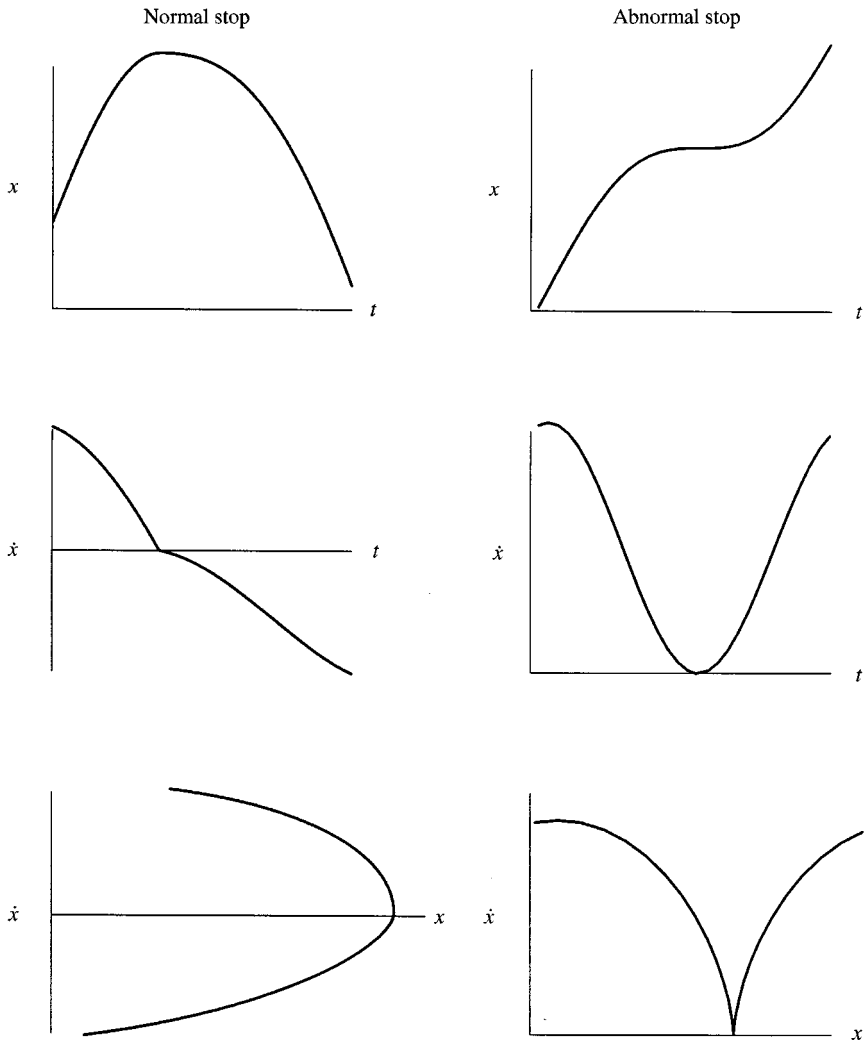


Figure 14. Stops with zero duration are divided into two types: normal stops and abnormal stops.

critical value α_c is calculated by

$$\alpha_c = \sqrt{\left(\frac{1}{\Omega^2} - 1\right)^2 \left[1 + \left(\frac{\Omega \sin \pi_1}{1 + \cos \pi_1}\right)^2\right]}, \tag{41}$$

which will be derived in reference [15]. In the range $\alpha < \alpha_c$, there exist abnormal stops before a turning point. For example, for the case of $(1/\alpha, \Omega) = (0.3, 0.012)$, $2\pi/\omega_d = 1$ s, there are two abnormal stops in the third cycle ($2 \leq t < 3$ s) as shown in Figure 16.

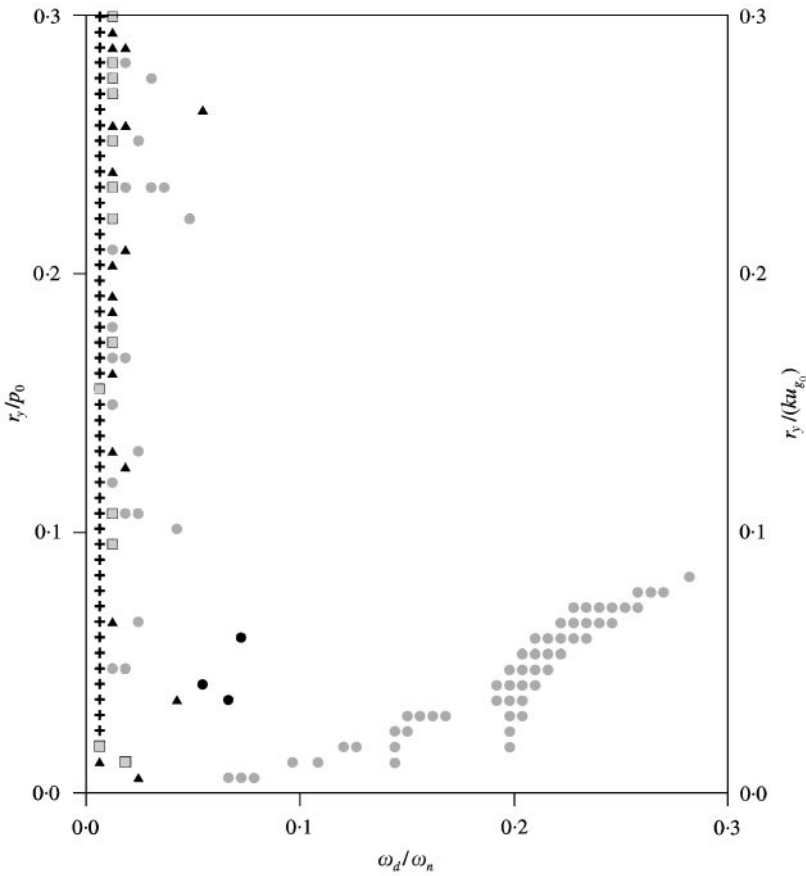


Figure 15. The distribution of the stops with zero duration in the range $0 < 1/\alpha < 0.3$ and $0 < \Omega < 0.3$. $1/\alpha = r_y/p_0$, $\Omega = \omega_d/\omega_n$: ●, normal stop; ▲, one abnormal stop; ■, two abnormal stops; +, more abnormal stops.

5. CONCLUSIONS

According to the above study we draw the following conclusions:

- (1) By verifying that equations (10)–(13) suffice to derive the conventional relations (7–9) but the converse is not true, we have shown that the conventional relations (7–9) is correct but incomplete, that Coulomb’s friction is described completely by equations (10–13), and that the relation between the constitutive force and displacement for the mass–spring–friction oscillator is described by equations (10–15). We have also shown that equations (10–13) have the higher-dimensional counterpart, equations (A1–A4).
- (2) Precise criteria for sliding and sticking have been derived in section 3.1. In most studies, this problem was treated as three phases, and correspondingly there were also three governing equations, one for each phase. In this paper, the complete and correct formulation has led to precisely two phases, sliding and sticking, resulting in more concise governing equations in terms of the

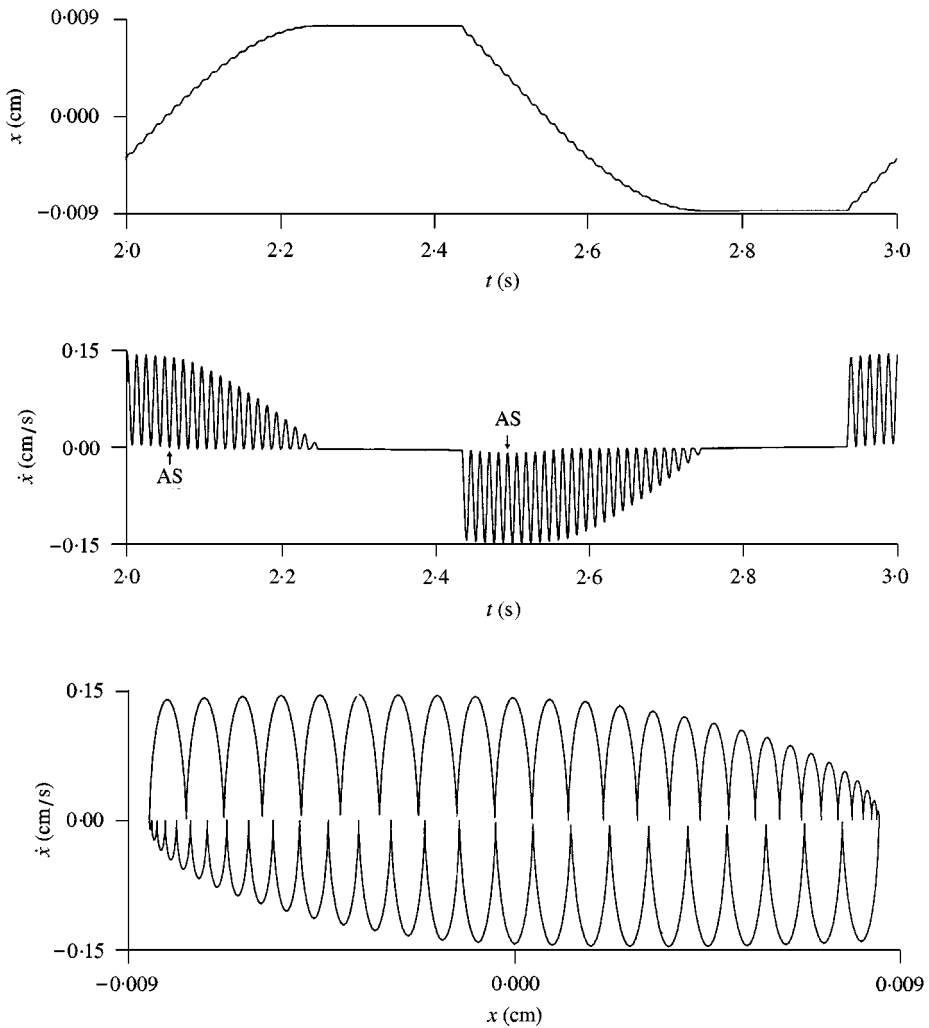


Figure 16. An example with two abnormal zero-duration stops (marked with AS) for $(1/\alpha, \Omega) = (0.3, 0.012)$.

position co-ordinate $x(t)$ and the constitutive force $r(t)$: equations (20) and (21) are the sliding-phase governing equations while equations (23) and (24) are the sticking-phase governing equations as well as exact solutions.

- (3) The simple formula (25) can identify a zero-duration stop and hence expresses the slide–slide condition, and, furthermore, the simple criteria (39) and (40) can distinguish between a normal zero-duration stop (39) and an abnormal zero-duration stop (40).
- (4) The above three conclusions apply to the Coulomb friction oscillator subjected to general loading. For simple harmonic loading we have obtained the exact solutions: equations (27) and (21) for the sliding phase, section 4.2 for the start-to-stick time, equations (23) and (24) for the sticking phase, and equations (30–36) for the start-to-slide time.

- (5) In the steady state the non-sticking oscillation (zero stop per cycle) and the sliding–sticking motion of a lower even number of stops per cycle have been found to be the typical (more frequently occurring) behavior of the harmonically excited friction oscillator. In the parametric space of ratios of force and frequency the behavior has been classified as in Figures 8 and 9.

REFERENCES

1. A. H. NAYFEH and D. T. MOOK 1979 *Nonlinear Oscillations*. New York: Wiley.
2. J. P. DEN HARTOG 1931 *Transactions of the American Society of Mechanical Engineers* **53**, 107–115. Forced vibrations with combined Coulomb and viscous friction.
3. R. A. IBRAHIM 1994 *Applied Mechanics Reviews* **47**, 209–253. Friction-induced vibration, chatter, squeal, and chaos. Part I: mechanics of contact and friction, Part II: dynamics and modeling.
4. A. SCHLESINGER 1979 *Journal of Sound and Vibration* **63**, 213–224. Vibration isolation in the presence of Coulomb friction.
5. R. PLUNKETT 1981 *Damping Applications for Vibration Control* (P. J. Torvik, ed.), AMD-Vol. 38, 65–75, New York: ASME. Friction damping.
6. T. K. PRATT and R. WILLIAMS 1981 *Journal of Sound and Vibration* **74**, 531–542. Non-linear analysis of stick/slip motion.
7. S. W. SHAW 1986 *Journal of Sound and Vibration* **108**, 305–325. On the dynamic response of a system with dry friction.
8. E. S. LEVITAN 1960 *Journal of the Acoustical Society of America* **32**, 1265–1269. Forced oscillation of a spring-mass system having combined Coulomb and viscous damping.
9. J. E. RUZICKA 1967 *Journal of Engineering for Industry* **89**, 729–740. Resonance characteristics of unidirectional viscous and Coulomb-damped vibration isolation systems.
10. J. J. MOREAU 1979 *Trends in Applications of Pure Mathematics to Mechanics*, (H. Zorski, ed.), Vol. 2, 263–280. London: Pitman. Application of convex analysis to some problems of dry friction.
11. N. MAKRIS and M. C. CONSTANTINO 1991 *Mechanics of Structure and Machine* **19**, 477–500. Analysis of motion resisted by friction: I. Constant Coulomb and linear Coulomb friction.
12. L. Y. CHEN , J. T. CHEN , C. H. CHEN and H.-K. HONG 1994 *Mechanics Research Communications* **21**, 599–604. Free vibration of a sdof system with hysteretic damping.
13. C.-S. LIU 1997 *Journal of the Chinese Institute of Engineers* **20**, 511–525. Exact solution and dynamic responses of SDOF bilinear elastoplastic structures.
14. R. I. SKINNER , W. H. ROBINSON and G. H. McVERRY 1993 *An Introduction to Seismic Isolation*. New York: Wiley.
15. H.-K. HONG and C.-S. LIU 1999 Non-sticking oscillation formulae for Coulomb friction under harmonic loading (submitted).

APPENDIX A: MULTI-DIMENSIONAL COULOMB FRICTION MODEL

It is difficult to extend the one-dimensional model of equations (7–9) to higher dimensions. However, the generalization of the model (10–13) to higher dimensions is rather straightforward as shown below:

$$\dot{\mathbf{x}} = (\dot{A}/r_y^2) \mathbf{r}_a, \quad (\text{A1})$$

$$\|\mathbf{r}_a\| \leq r_y, \quad (\text{A2})$$

$$\dot{A} \geq 0, \quad (\text{A3})$$

$$\|\mathbf{r}_a\| \dot{A} = \mathbf{r}_y \dot{A}, \quad (\text{A4})$$

where $\|\mathbf{r}_a\|$ is the Euclidean norm of \mathbf{r}_a and \mathbf{r}_a and \mathbf{x} are the $n \times 1$ matrices of friction force and displacement, respectively, of the oscillator.

It is clear that equation (A1) may be replaced by

$$\dot{\mathbf{x}} = \dot{\lambda} \mathbf{r}_a, \quad (\text{A5})$$

where $\dot{\lambda}$ is a proportional multiplier with

$$\lambda = l/r_y = A/r_y^2, \quad (\text{A6})$$

l being the sliding length and A dissipated energy due to friction. From equations (A3) and (4-6) we have $\dot{\lambda} \geq 0$ and $\dot{l} \geq 0$, the latter of which means the sliding length is never decreasing, an obvious fact yet an indispensable ingredient for modelling.